Adaptive Control with MRAC Regulator for DC-DC Buck Converter

AHMED CHOUYA
University of Djilali Bounâama
Department of Genie Electrical
Khemis-Miliana City, 44 225
ALGERIA

KADA BOUREGUIG
University of Ibn-Khaldoun
Department of Mechanical Engineering
Tiaret City, 14 000
ALGERIA

Abstract: In this article; we process DC-DC buck converter by adaptive controller. The Massachusetts Institute of Technology (MIT) rule is applied as an adaptive mechanism to determine the optimum control parameters under certain conditions. The regulators take three positions; it located in: - feed forward and direct chain; - feed forward and feed back; -direct chain and feed back. The adaptive control technique used is Model Reference Adaptive Control (MRAC); this method can control the system by varying the output voltages, input voltage and load resistance. The proposed method has a stable response capable of reaching the model reference smoothly.

Key–Words: DC-DC Buck Converter, Model Reference Adaptive Control (MRAC), Massachusetts Institute of Technology (MIT) Rule.

Received: May 10, 2021. Revised: February 13, 2022. Accepted: February 21, 2022. Published: April 1, 2022.

1 Introduction

Power electronics is part of electrical engineering which deals with the static conversion of electrical energy from one form to another, adapted to the user's needs. The systems responsible for managing electrical energy are static converters which make it possible to adapt the electrical source of energy to a given receiver in conversion between the network and the load. DC-DC converters are a fairly important part of the conversion chain. They are widely used in connections to accumulator batteries, photovoltaic systems, wind turbines, hybrid systems in [11].

The classical non isolated DC-DC converters, which include the buck, boost, buck-boost, Cuk, SEPIC (Single Ended Primary Inductance Converter) and Zeta (dual-SEPlC) topologies are inadequate for high-power applications, since only one active switch and one diode are responsible for processing the load power.

There are two main approaches presented by the literature. The first Linear duty cycle control based on Proportional Integral Derivative compensation (PID) (see [3, 8, 1, 4, 5, 9]). Several works have based their control strategy on voltage control using type PI (or type II) compensation. Other work (looking for a higher bandwidth) adds the function derived by adding a zero to the PI control, forming the PID (or type III) or by using the second loop based on a control in current (see. [14, 7]). The second is Nonlinear controls such as control V^2 in [16], hysteretic control in [12, 2], Sliding mode control or even Boundary control. The most used is the hysteretic control which can be carried out either by voltage detection or current detection. [13]'s work presents the design of a 3-state Buck converter to improve the dynamic behaviour of microprocessor supply voltages.

In this article ; we are going to apply the MIT rule on a Buck converter. The next section will be the modeling of the Buck followed by the synthesis of the command. the results and simulations will be in the fourth section and the conclusion in the fift section.

2 DC-DC Buck Converter Model

The electrical circuit of the buck converter is presented in the figure1

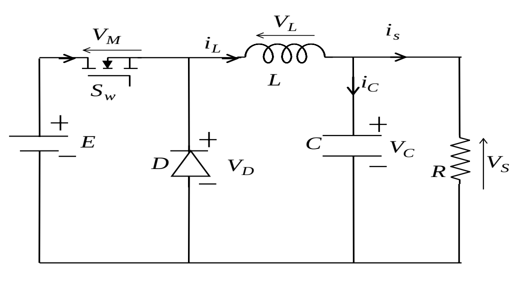

Figure 1: Buck converter diagram.

The equivalent circuit of the buck converter shown in figur 1 is :

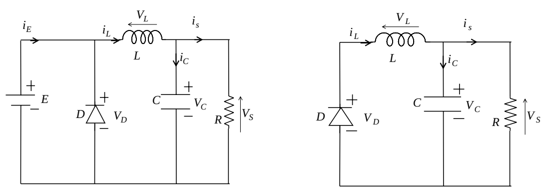

Figure 2: Schematic of the buck converter with S_w closed (left) and S_w opened (right)

During the interval, $t_0 \leq t \leq t_0 + \alpha T$, the switch S_w is closed and the diode D is blocked. The linear model which represents the left configuratio of the circuit describes in figur 2 is given by :

$$\begin{bmatrix} \frac{di_L}{dt} \\ \\ \frac{dV_C}{dt} \end{bmatrix} = \begin{bmatrix} 0 & -\frac{1}{L} \\ \\ \frac{1}{C} & -\frac{1}{RC} \end{bmatrix} \begin{bmatrix} i_L \\ \\ V_C \end{bmatrix} + \begin{bmatrix} \frac{1}{L} \\ \\ 0 \end{bmatrix} E \tag{1}$$

Over the interval, $t_0 + \alpha T \leq t \leq t_0 + T$, S_w is open and the diode D is conducting. The linear model which represents the good configuratio of the circuit described in the figur 2 is given by :

$$\begin{bmatrix} \frac{di_L}{dt} \\ \\ \frac{dV_C}{dt} \end{bmatrix} = \begin{bmatrix} 0 & -\frac{1}{L} \\ \\ \frac{1}{C} & -\frac{1}{RC} \end{bmatrix} \begin{bmatrix} i_L \\ \\ V_C \end{bmatrix} + \begin{bmatrix} 0 \\ \\ 0 \end{bmatrix} E \tag{2}$$

The state space mean model for the buck converter is shown in equation (3).

$$\begin{bmatrix} \frac{di_L}{dt} \\ \\ \frac{dV_C}{dt} \end{bmatrix} = \begin{bmatrix} 0 & -\frac{1}{L} \\ \\ \frac{1}{C} & -\frac{1}{RC} \end{bmatrix} \begin{bmatrix} i_L \\ \\ V_C \end{bmatrix} + \begin{bmatrix} \frac{\alpha}{L} \\ \\ 0 \end{bmatrix} E \tag{3}$$

From $V_C = V_s$; we fin the firs transfer function linking the output voltage V_s with the duty cyclic α:

$$\frac{V_s(s)}{\alpha(s)} = \frac{E}{LC} . \frac{1}{s^2 + \frac{1}{RC}s + \frac{1}{LC}} \tag{4}$$

We deduce the transfer function linking the inductor current i_L with the duty cyclic α:

$$\frac{i_L(s)}{\alpha(s)} = \frac{E}{L} . \frac{s + \frac{1}{RC}}{s^2 + \frac{1}{RC}s + \frac{1}{LC}} \tag{5}$$

3 Synthesis of Adaptive Control with MRAC Regulator

According to the firs equation of expression (3); we can deduce the control law according to:

$$\alpha = \frac{L}{E} s i_L + \frac{V_s}{E} \tag{6}$$

Massachusetts Institute of Technology (MIT) rule is:

$$\mathcal{L}\left\{\frac{d\theta}{dt}\right\} = -\gamma \frac{\partial J(e)}{\partial e} \frac{\partial e}{\partial \theta} \tag{7}$$

Where e represents the error between the plant and model output. The θ is adjustable parameter and it is set in such a way such that J is minimized to zero.

That is to say the optimality criterion $J(e)$ of the adjustment loop is expressed by the absolute value (see [15] and [6]):

$$J(e) = |e| \tag{8}$$

Its derivative is :

$$\frac{\partial J(e)}{\partial e} = sign(e) \tag{9}$$

We will present the synthesis of each regulator separately closely connected to clarify the methodology of synthesis of each one of them.

3.1 Output Voltage Regulator Located at Feed Forward and Direct Chain

To achieve this objective, one takes an MRAC of the type:

$$I_L(s) = (\theta_1 V_{ref}(s) - V_s(s))\,\theta_2 \tag{10}$$

We can represent the closed loop system by the figur 3.

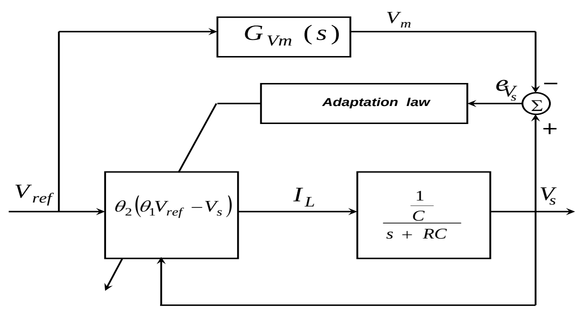

Figure 3: MRAC closed loop circuit diagram block of output voltage.

The reference model of the closed loop system is selected with a firs order transfer function:

$$G_m(s) = \frac{b_m}{s + a_m}$$

In closed loop, the transfer function is written:

$$G_{BF1}(s) = \frac{\theta_1\theta_2K_C}{s + RC + \theta_2K_C} \qquad (11)$$

With $K_C = \frac{1}{C}$. The error $e = V_s - V_m$, its derivative compared to the parameters gives :

$$\frac{\partial e}{\partial \theta_1} = \frac{\theta_2K_C}{s + RC + \theta_2K_C}V_{ref}(s) \qquad (12)$$

$$\begin{aligned}\frac{\partial e}{\partial \theta_2} &= \frac{\theta_1K_C}{s + RC + \theta_2K_C}V_{ref}(s)\\ &\quad -\frac{\theta_1\theta_2K_C^2}{(s + RC + \theta_2K_C)^2}V_{ref}(s)\end{aligned} \qquad (13)$$

For $e = 0 \Rightarrow V_s = V_m$ then $RC + \theta_2K_C = a_m$ and $\theta_1\theta_2K_C = b_m$.

$$\frac{\partial e}{\partial \theta_1} = \frac{1}{\theta_1}.\frac{b_m}{s + a_m}V_{ref}(s) = \frac{1}{\theta_1}.V_m(s) \qquad (14)$$

$$\begin{aligned}\frac{\partial e}{\partial \theta_2} &= \frac{1}{\theta_2}.\frac{b_m}{s + a_m}V_{ref}(s) - \frac{1}{\theta_1\theta_2}.\frac{b_m}{s + a_m}\\ &\quad .\frac{b_m}{s + a_m}V_{ref}(s)\\ &= \frac{1}{\theta_2}.\frac{b_m}{s + a_m}.\left(V_{ref}(s) - \frac{1}{\theta_1}V_m(s)\right)\end{aligned} \qquad (15)$$

Taking into account (9), (14) and (15), one can write the gradient equation θ_1 and θ_2:

$$\mathcal{L}\left\{\frac{d\theta_1}{dt}\right\} = -\gamma_1\frac{\partial J(e)}{\partial e}\frac{\partial e}{\partial \theta_1} \qquad (16)$$

$$\theta_1(s) = -\frac{\gamma_1}{s}sign(e).\frac{1}{\theta_1}.V_m(s) \qquad (17)$$

And

$$\mathcal{L}\left\{\frac{d\theta_2}{dt}\right\} = -\gamma_2\frac{\partial J(e)}{\partial e}\frac{\partial e}{\partial \theta_2} \qquad (18)$$

$$\begin{aligned}\theta_2 &= -\frac{\gamma_2}{s}sign(e).\frac{1}{\theta_2}.\frac{b_{Vm}}{s + a_{Vm}}\\ &\quad .\left(V_{ref}(s) - \frac{1}{\theta_1}V_m(s)\right)\end{aligned} \qquad (19)$$

3.2 Output Voltage Regulator Located at Feed Forward and Feed Back

The equation for this type of regulator is given by:

$$I_L(s) = \rho_1V_{ref}(s) - \rho_2V_s(s) \qquad (20)$$

The closed loop of expression (20) will be presented in figur 4.

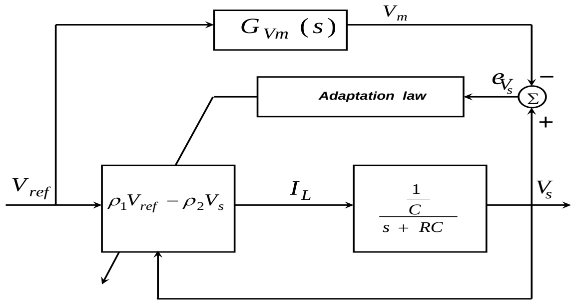

Figure 4: MRAC closed loop circuit diagram block of output voltage.

Closed loop; the transfer function of the system is given by:

$$G_{BF2}(s) = \frac{\rho_1K_C}{s + RC + \rho_2K_C} \qquad (21)$$

The error $e = V_s - V_m$, Their derivatives compared to the parameters ρ_1 and ρ_2 are: :

$$\frac{\partial e}{\partial \rho_1} = \frac{K_C}{s + RC + \rho_2K_C}V_{ref}(s) \qquad (22)$$

$$\frac{\partial e}{\partial \rho_2} = -\frac{\rho_1K_C^2}{(s + RC + \rho_2K_C)^2}V_{ref}(s) \qquad (23)$$

when the error is zero $e = 0 \Rightarrow V_s = V_m$ then $RC + \rho_2K_C = a_m$ and $\rho_1K_C = b_m$.

$$\frac{\partial e}{\partial \rho_1} = \frac{1}{\rho_1}.\frac{b_m}{s + a_m}V_{ref}(s) = \frac{1}{\rho_1}.V_m(s) \qquad (24)$$

$$\begin{aligned}\frac{\partial e}{\partial \rho_2} &= -\frac{1}{\rho_1}.\frac{b_m}{s + a_m}.\frac{b_m}{s + a_m}V_{ref}(s)\\ &= -\frac{1}{\rho_1}.\frac{b_m}{s + a_m}.V_m(s)\end{aligned} \qquad (25)$$

Taking ; consideration (9), (24) and (25), the equation gradient ρ_1 and ρ_2 are :

$$\mathcal{L}\left\{\frac{d\rho_1}{dt}\right\} = -\gamma_1\frac{\partial J(e)}{\partial e}\frac{\partial e}{\partial \rho_1} \qquad (26)$$

$$\rho_1(s) = -\frac{\gamma_1}{s}sign(e).\frac{1}{\rho_1}.V_m(s) \qquad (27)$$

And

$$\mathcal{L}\left\{\frac{d\rho_2}{dt}\right\} = -\gamma_2\frac{\partial J(e)}{\partial e}\frac{\partial e}{\partial \rho_2} \quad (28)$$

$$\rho_2 = \frac{\gamma_2}{s}sign(e).\frac{1}{\rho_1}.\frac{b_m}{s+a_m}.V_m(s) \quad (29)$$

3.3 Output Voltage Regulator Located at Direct Chain and Feed Back

In this case the regulator formula is :

$$I_L(s) = \varrho_1\left(V_{ref}(s) - \varrho_2 V_s(s)\right) \quad (30)$$

The closed loop system is shown in the figur 5.

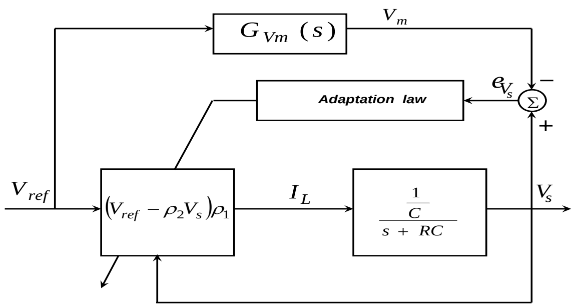

Figure 5: MRAC closed loop circuit diagram block of output voltage.

In closed loop, the transfer function is written:

$$G_{BF3}(s) = \frac{\varrho_1 K_C}{s + RC + \varrho_1\varrho_2 K_C} \quad (31)$$

The error $e = V_s - V_m$, its derivative compared to the parameters gives :

$$\frac{\partial e}{\partial \varrho_1} = \frac{1}{\varrho_1}.\frac{\varrho_1 K_C}{s+RC+\varrho_1\varrho_2 K_C}V_{ref}(s) - \frac{1}{\varrho_1}.\frac{\varrho_1^2\varrho_2 K_C^2}{(s+RC+\varrho_1\varrho_2K_C)^2}V_{ref}(s) \quad (32)$$

$$\frac{\partial e}{\partial \varrho_2} = -\frac{\varrho_1^2 K_C^2}{(s+RC+\varrho_1\varrho_2K_C)^2}V_{ref}(s) \quad (33)$$

According to equations (9), (32) and (33), the gradient ϱ_1 and ϱ_2 of the formula :

$$\mathcal{L}\left\{\frac{d\varrho_1}{dt}\right\} = -\gamma_1\frac{\partial J(e)}{\partial e}\frac{\partial e}{\partial \varrho_1} \quad (34)$$

$$\varrho_1(s) = -\frac{\gamma_1}{s}.\frac{1}{\varrho_1}\left(1-\varrho_2.\frac{b_m}{s+a_m}\right).V_m .sign(e) \quad (35)$$

And

$$\mathcal{L}\left\{\frac{d\varrho_2}{dt}\right\} = -\gamma_2\frac{\partial J(e)}{\partial e}\frac{\partial e}{\partial \varrho_2} \quad (36)$$

$$\varrho_2 = \frac{\gamma_2}{s}sign(e).\frac{b_m}{s+a_m}.V_m(s) \quad (37)$$

3.4 Inductor Current Regulator

For the closed loop inductance current, an MRAC regulator of the form has been proposed:

$$\alpha = \vartheta_2\left(\vartheta_1 I_{ref}(s) - I_L(s)\right) \quad (38)$$

The functional diagram is given by the figur 6.

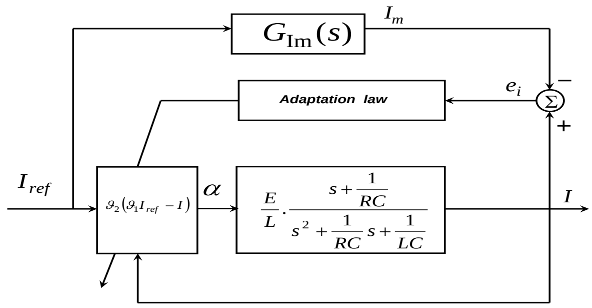

Figure 6: Schematic block in loop closed of inductor current MRAC regulator.

If the desired mean tension with equilibrium is $V_{seq} = V_d$, then we have with equilibrium $i_{Leq} = \frac{V_d}{R} = I_{ref}$ et $\alpha_{eq} = \frac{V_d}{E}$.
The reference model of the loop closed is selected with a second-order transfer function:

$$G_{Im}(s) = \frac{b_{1im}s + b_{0im}}{s^2 + a_{1im}s + a_{0im}}$$

In open loop, the transfer function is written:

$$G_{BOi}(s) = \frac{\vartheta_1\vartheta_2\frac{E}{L}\left(s+\frac{1}{RC}\right)}{s^2+\frac{1}{RC}s+\frac{1}{LC}} \quad (39)$$

And in closed loop:

$$G_{BFi}(s) = \frac{\vartheta_1\vartheta_2\frac{E}{L}\left(s+\frac{1}{RC}\right)}{s^2+\left(\frac{1}{RC}+\frac{E\vartheta_2}{L}\right)s+\left(\frac{E\vartheta_2}{RLC}+\frac{1}{LC}\right)} \quad (40)$$

The error $e = I - I_m$, its derivative compared to the parameters gives :

$$\frac{\partial e}{\partial \vartheta_1} = \frac{\vartheta_2 \frac{E}{L}\left(s + \frac{1}{RC}\right)}{s^2 + \left(\frac{1}{RC} + \frac{E\vartheta_2}{L}\right)s + \left(\frac{E\vartheta_2}{RLC} + \frac{1}{LC}\right)} I_{ref} \quad (41)$$

$$\frac{\partial e}{\partial \vartheta_2} = \frac{\vartheta_1 \frac{E}{L}\left(s + \frac{1}{RC}\right)}{s^2 + \left(\frac{1}{RC} + \frac{E\vartheta_2}{L}\right)s + \left(\frac{E\vartheta_2}{RLC} + \frac{1}{LC}\right)} I_{ref} - \frac{\vartheta_1\vartheta_2 \frac{E^2}{L^2}\left(s + \frac{1}{RC}\right)^2}{\left(s^2 + \left(\frac{1}{RC} + \frac{E\vartheta_2}{L}\right)s + \left(\frac{E\vartheta_2}{RLC} + \frac{1}{LC}\right)\right)^2} I_{ref}(s) \quad (42)$$

So that $e = 0 \Rightarrow I = I_m$ then $\frac{E\vartheta_2}{RLC} + \frac{1}{LC} = a_{0im}$; $\frac{1}{RC} + \frac{E\vartheta_2}{L} = a_{1im}$; $\vartheta_1\vartheta_2\frac{E}{L} = b_{1im}$ and $\vartheta_1\vartheta_2\frac{E}{RLC} = b_{0im}$.

$$\begin{aligned} \frac{\partial e}{\partial \vartheta_1} &= \frac{1}{\vartheta_1}.\frac{b_{1im}s + b_{0im}}{s^2 + a_{1im}s + a_{0im}} I_{ref}(s) \\ &= \frac{1}{\vartheta_1}.I_m(s) \end{aligned} \quad (43)$$

$$\begin{aligned} \frac{\partial e}{\partial \vartheta_2} &= \frac{1}{\vartheta_2}.\frac{b_{1im}s + b_{0im}}{s^2 + a_{1im}s + a_{0im}} I_{ref}(s) \\ &\quad - \frac{1}{\vartheta_1\vartheta_2}.\left(\frac{b_{1im}s + b_{0im}}{s^2 + a_{1im}s + a_{0im}}\right)^2 I_{ref}(s) \\ &= \frac{1}{\vartheta_2}.\frac{b_{1im}s + b_{0im}}{s^2 + a_{1im}s + a_{0im}} \\ &\quad .\left(I_{ref}(s) - \frac{1}{\vartheta_1} I_m(s)\right) \end{aligned} \quad (44)$$

Taking into account (9), (43) and (44), one can write the equation of gradient ϑ_1 and ϑ_2:

$$\mathcal{L}\left\{\frac{d\vartheta_1}{dt}\right\} = -\gamma_{i1}\frac{\partial J(e)}{\partial e}\frac{\partial e}{\partial \vartheta_1} \quad (45)$$

$$\vartheta_1 = -\frac{\gamma_{i1}}{s}.sign(e).\frac{1}{\vartheta_1}.I_m(s) \quad (46)$$

And

$$\mathcal{L}\left\{\frac{d\vartheta_2}{dt}\right\} = -\gamma_{i2}\frac{\partial J(e)}{\partial e}\frac{\partial e}{\partial \vartheta_2} \quad (47)$$

$$\begin{aligned} \vartheta_2 &= -\frac{\gamma_{i2}}{s} sign(e).\frac{1}{\vartheta_2}.\frac{b_{1im}s + b_{0im}}{s^2 + a_{1im}s + a_{0im}} \\ &\quad .\left(I_{ref}(s) - \frac{1}{\vartheta_1} I_m(s)\right) \end{aligned} \quad (48)$$

4 Results and Simulations

This work is based on the output voltage and inductance current generated by the Buck converter which has adaptive regulation. See this when there are changes in the output voltage, input voltage, and resistance load. This research that will be carried out in a buck converter using a adaptive controller when :

- Output voltage regulator located at feed forward and direct chain;
- Output voltage regulator located at feed forward and feed back;
- Output voltage regulator located at direct chain and feed back.

And inductor current regulator located at feed forward and direct chain with a buck converter using MRAC. To examine practical usefulness, the proposed regulator has been simulated for a Buck (see [10]), whose parameters are depicted in Table 1.

Table 1: DC-DC buck converter parameters.([10])

Parameters	Notation	Value	Unit
Input Voltage	E	24	V
Output Voltage	V_s	12	V
Inductance	L	69	μH
Resistance Load	R	13	Ω
Capacitor	C	220	μF
Normal switching frequency	f	100	KHz
Switch off	Sw	$\alpha = 0$	
Switch off	Sw	$\alpha = 1$	

By using these parameters, the model of DC-DC buck converter (3) is utilized as a plant of the system. The MRAC based on ***MIT*** rule for inductor output voltage Regulator obtain :

Equations (17) and (19) for output voltage regulator located at feed forward and direct chain;

Equations (27) and (29) for output voltage regulator located at feed forward and feed back;

Equations (35) and (37) for output voltage regulator located at direct chain and feed back.

And current regulator (46) and (48). The value of γ is specifie to achieve the appropriate response.

We show a detailed general diagram of adaptive control with MRAC regulator in the figur 7.

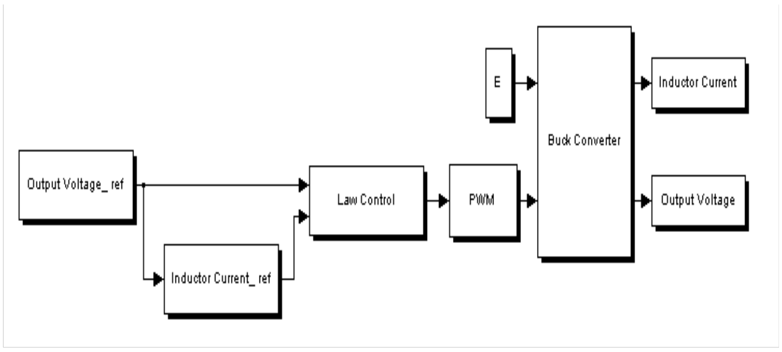

Figure 7: General diagram of adaptive control with MRAC regulator for DC-DC buck converter.

The performance of buck converter in proposed controller is proven in simulation such that any changed responses are able to be observed. The input voltage and resistor load of the buck converter are $24V$ and 13Ω, respectively. Reference voltage is set to be $12V$ and of γ as following: $\begin{bmatrix} \gamma_{V1} & \gamma_{V2} & \gamma_{i1} & \gamma_{i2} \end{bmatrix} = \begin{bmatrix} 250 & 500 & 1.5 & 650 \end{bmatrix}$. As regulation parameters are initialized to $\begin{bmatrix} \theta_1 & \theta_2 & \rho_1 & \rho_2 & \varrho_1 & \varrho_2 & \vartheta_1 & \vartheta_2 \end{bmatrix} = \begin{bmatrix} 1 & 47 & 1 & 47 & 1 & 4.7 & 61 & 0.64 \end{bmatrix}$.

Change in reference output voltage:
The desired output voltage is set to $12V$; at the instant $t = 0.08s$, it is changed to $17V$. Figure 8 represents the output voltage error and its histogram with the assembly Gaussian; distribution given by figur 3. There are oscillations at start-up, the peak error $5.53V$, at the instant of variation the desired voltage with a peak error of $66.6 \times 10^{-2}V$. the mean error is $-21.03 \times 10^{-2}V$ and the variance 38.42×10^{-2}. The development of duty cycle α is shown in figur 9 where it takes the values 0.5 then 7×10^{-1}. The evolution of adaptation gains is presented in figur 10(a) and 10(b) where $\theta_1 = 1$ and $\theta_2 = 4.699 \times 10^1$.

When we have the assembly of figur 4. The peak error, at start-up, is $8.543V$ and $0.54V$ at the time of variation of the voltage (see figur 11). $-0.2577V$ is the mean of output voltage error and 1.8177 variance. Figure 12 configure the duty cycle where α is 0.5 then 7×10^{-1}. The shape of the apparent adaptation gains is shown in figur 13 with $\rho_1 = 2.841$ and $\rho_2 = 20.84 \times 10^{-1}$.

For the diagram in figur 5. $-12.25V$ is the peak output voltage error at start-up and reaches $3.0212V$ during the voltage variation (figur 14). The mean output voltage error is $-0.3558V$ with the variance 518.18×10^{-2}. α equals 0.5 and 0.7 are the duty cycles following the change in the desired voltage (Figure 15). The shape of the apparent adaptation gains is shown in figur 16 with $\varrho_1 = 1$ and $\varrho_2 = 1$.

The inductor current is given by the figur 17(a). We notice that there are oscillations along the desired trajectory but it follows it. The evolution of the correction gain ϑ_1 and ϑ_2 are given by the figur 17(b); where $\vartheta_1 = 60.99$ and $\vartheta_2 = 64.9 \times 10^{-2}$. The inductor current error and the histogram with Gaussian distribution are shown by figure 18(a) and 18(b) respectively. The error means is equal $0.3714A$ and the variance is 12.654×10^{-1}.

Change in input voltage:
The input voltage is set to $24V$; at the instant $t = 0.08s$, it is changed to $29V$. Figure 19 represents the output voltage error and its histogram with the Gaussian distribution; assembly given by figur 3. There are oscillations at start-up, the peak error $5.53V$, at the instant of variation the desired voltage with a peak error of $66.6 \times 10^{-2}V$. the mean error is $-16.34 \times 10^{-2}V$ and the variance 38.47×10^{-2}. The development of duty cycle α is shown in figur 20 where it takes the values 0.5 then 4×10^{-1}. The evolution of adaptation gains is presented in figur 21(a) and 21(b) where $\theta_1 = 1$ and $\theta_2 = 4.699 \times 10^1$.

When we have the assembly of figur 4. The peak error, at start-up, is $8.919V$ and $0.298V$ at the time of variation of the input voltage (see figur 22). $-17.94 \times 10^{-2}V$ is the mean of output voltage error and 164.81×10^{-2} variance. Figure 23 configure the duty cycle where α is 0.5 then 41.38×10^{-2}. The shape of the apparent adaptation gains is shown in fig ure 24 with $\rho_1 = 2.841$ and $\rho_2 = 28.4 \times 10^{-1}$.

For the diagram in figur 5. $-6.251V$ is the peak output voltage error at start-up and reaches $0.4472V$ during the input voltage variation (figur 25). The mean output voltage error is $-0.2085V$ with the variance 34.20×10^{-2}. α equals 0.5 and 0.416 are the duty cycles following the change in the desired voltage (Figure 26). The shape of the apparent adaptation gains is shown in figur 27 with $\varrho_1 = 1.4955$ and $\varrho_2 = 1$.

In figur 28(a), the inductor current oscillated along the desired trajectory but it follows it. The evolution of the correction gain ϑ_1 and ϑ_2 are given by the figur 28(b); where $\vartheta_1 = 60.99$ and $\vartheta_2 = 64.9 \times 10^{-2}$. The inductor current error and the histogram with Gaussian distribution are shown by figure 29(a) and 29(b) respectively. The error means is equal $0.3028A$ and the variance is 12.595×10^{-1}.

Change in the resistor load:
The resistor load is set to 13Ω; at the instant $t = 0.08s$, it is changed to 26Ω. Figure 30 represents the output voltage error and its histogram with the Gaussian distribution; assembly given by figur 3. There are oscillations at start-up, the peak error $4.8562V$, at the instant of variation the desired voltage with a peak error of $-17.07 \times 10^{-1}V$;$1.3387x10^5$. the mean error is -0.1886 and the variance 21.86×10^{-2}. The development of duty cycle α is shown in figur 31 where it takes the values 5×10^{-1}. The evolution of adaptation gains is presented in figur 32(a) and 32(b) where $\theta_1 = 1$ and $\theta_2 = 4.699 \times 10^1$.

When we have the assembly of figur 4. The peak error, at start-up, is $8.9188V$ and $-1.7168V$ at the time of variation of the input voltage (see figur 33). $-0.2182V$ is the mean of output voltage error and 1.6684 variance. Figure 34 configure the duty cycle where α is 0.5. The shape of the apparent adaptation gains is shown in figur 35 with $\rho_1 = 2.841$ and $\rho_2 = 28.4 \times 10^{-1}$.

For the diagram in figur 5. V is the peak output voltage error at start-up and reaches 11 during the input voltage variation (figur 36). The mean output voltage error is $-0.1746V$ with the variance 35.38×10^{-2}. α equals 0.5 is the duty cycles following the change in the desired voltage (Figure 37). The shape of the apparent adaptation gains is shown in figur 38 with $\varrho_1 = 1.4955$ and $\varrho_2 = 1$.

The inductor current oscillated along the desired trajectory but it follows it (Figure39(a)). The evolution of the correction gain ϑ_1 and ϑ_2 are given by the figur 39(b); where $\vartheta_1 = 60.99$ and $\vartheta_2 = 65 \times 10^{-2}$. The inductor current error and the histogram with Gaussian distribution are shown by figure 40(a) and 40(b) respectively. The error means is equal $0.2011A$ and the variance is 9.605×10^{-1}.

Table 2: Means and variances of output voltage error for regulator located at feed forward and direct Chain.

Change in	output voltage	input voltage	resistor load
Mean	$0.2103V$	$0.1634V$	$0.1886V$
Var	0.3842	0.3847	0.2186

Table 3: Means and variances of output voltage error for regulator located at feed forward and feed back.

Change in	output voltage	input voltage	resistor load
Mean	$0.2577V$	$0.1794V$	$0.2182V$
Var	1.817	1.6481	1.6684

Table 4: Means and variances of output voltage error for regulator located at direct chain and feed back.

Change in	output voltage	input voltage	resistor load
Mean	$0.3558V$	$0.2085V$	$0.1746V$
Var	5.1818	0.3420	0.3538

Table 5: Means and variances of inductor current error.

Change in	output voltage	input voltage	resistor load
Mean	0.371	0.3028	0.2011
Var	1.2654	31.2595	0.9605

The table 2, table 3, table 4 and table 5 are collection of the preceding results. We notice :

- For the regulator located at the feed forward and direct chain, the change to the input voltage gives a minimum error means.
- For the regulator located at feed forward and feedback, the change to the input voltage gives a minimum error means.

- For the regulator located in the direct and feed back chain, changing the load resistance gives the best result.

The smaller mean value obtained, in these assemblies, in the case of the regulator located at the feed forward and direct chain, the change to the input voltage.

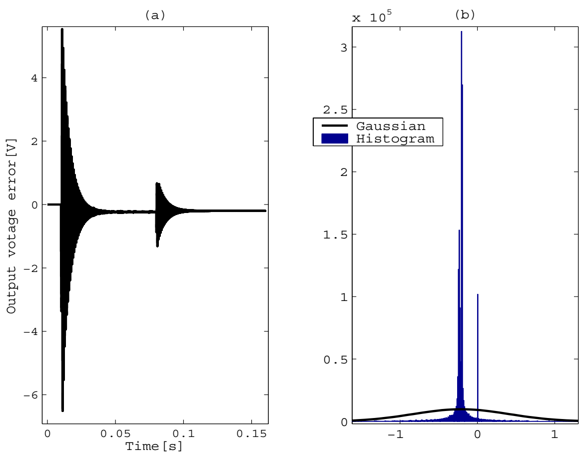

Figure 8: Output voltage error with histogram and Gaussian distribution for change in reference output voltage and regulator located at feed forward and direct chain.

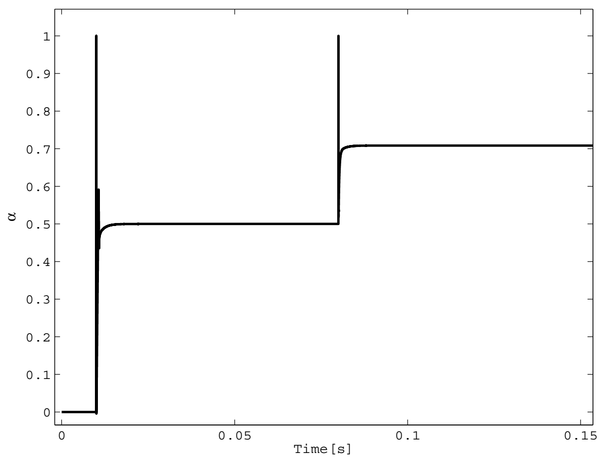

Figure 9: Duty cyclic α for change in reference output voltage and regulator located at feed forward and direct chain.

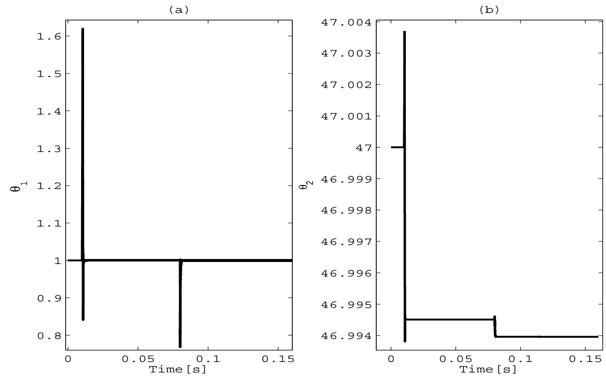

Figure 10: Evolution of adaptation gains θ_1 and θ_2 for change in reference output voltage and regulator located at feed forward and direct chain.

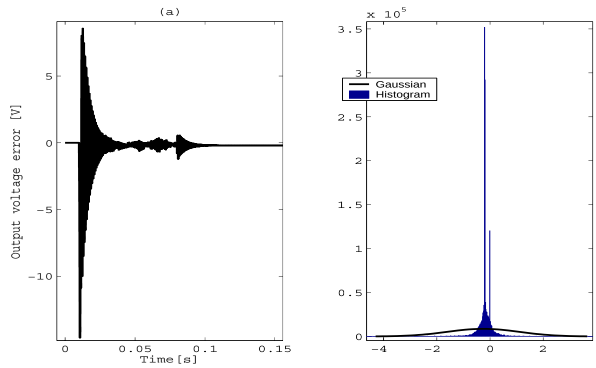

Figure 11: Output voltage error with histogram and Gaussian distribution for change in reference output voltage and regulator located at feed forward and feed back.

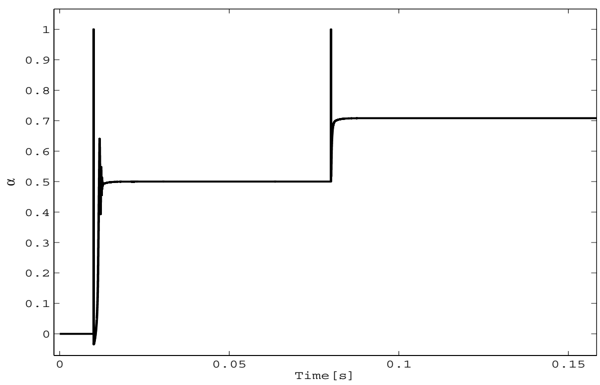

Figure 12: Duty cyclic α for change in reference output voltage and regulator located at feed forward and feed back.

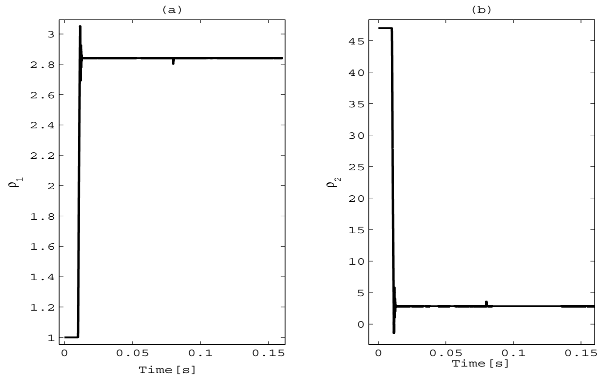

Figure 13: Evolution of adaptation gains ρ_1 and ρ_2 for change in reference output voltage and regulator located at feed forward and feed back.

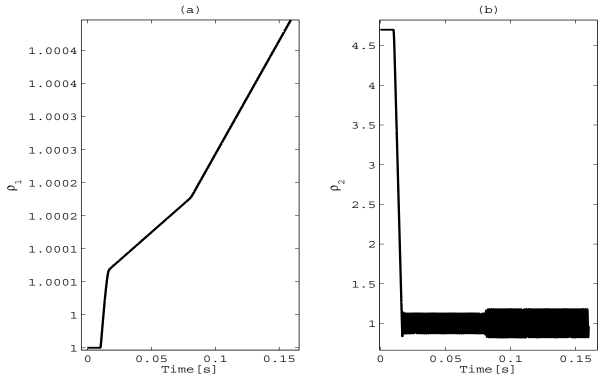

Figure 16: Evolution of adaptation gains ϱ_1 and ϱ_2 for change in reference output voltage and regulator located at direct chain and feed back.

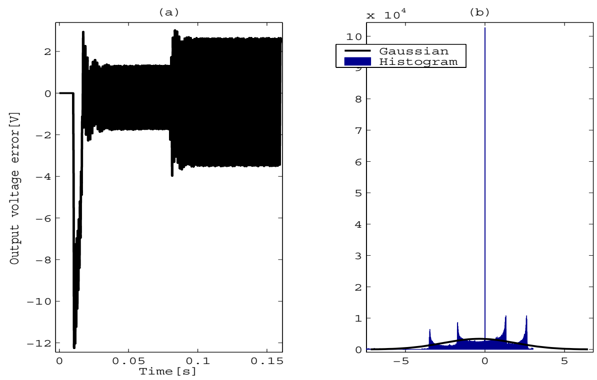

Figure 14: Output voltage error with histogram and Gaussian distribution for change in reference output voltage and regulator located at direct chain and feed back.

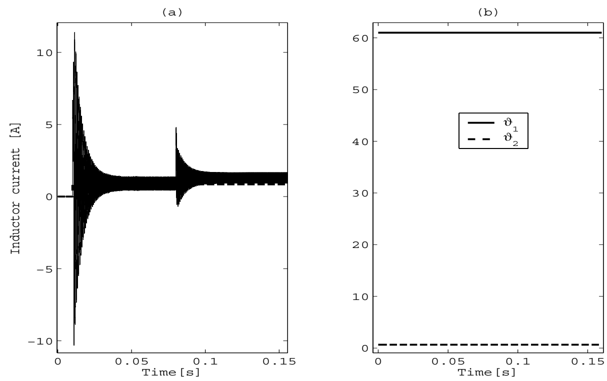

Figure 17: Inductor current with Evolution of ϑ_1 and ϑ_2.

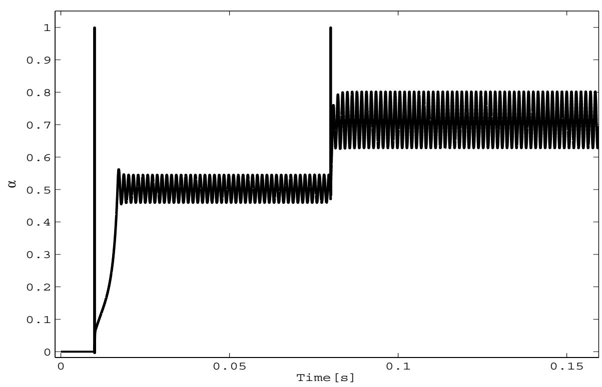

Figure 15: Duty cyclic α for change in reference output voltage and regulator located at direct chain and feed back.

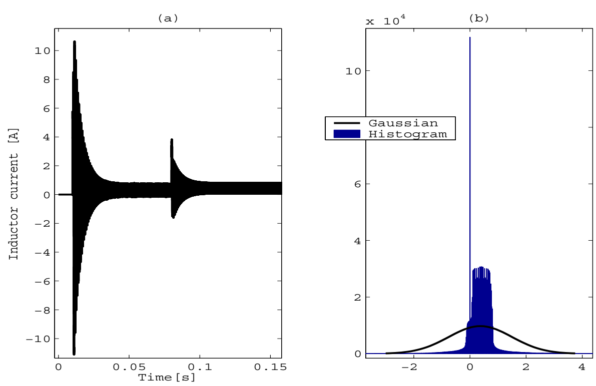

Figure 18: Inductor current error with histogram and Gaussian distribution.

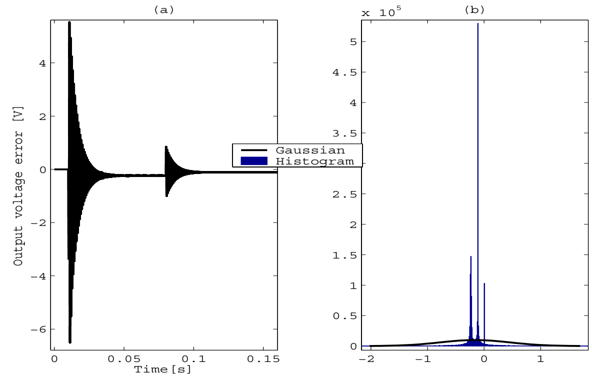

Figure 19: Output voltage error with histogram and Gaussian distribution for change in input voltage and regulator located at feed forward and direct chain.

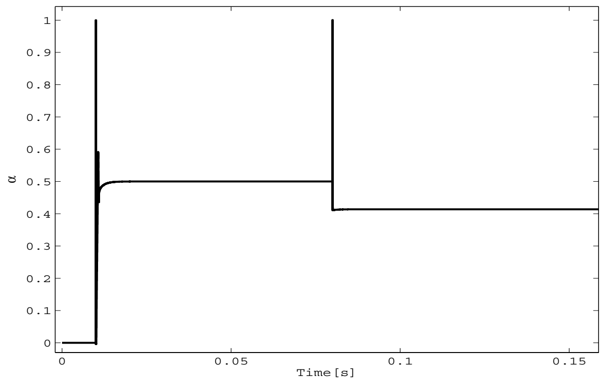

Figure 20: Duty cyclic α for change in input voltage and regulator located at feed forward and direct chain.

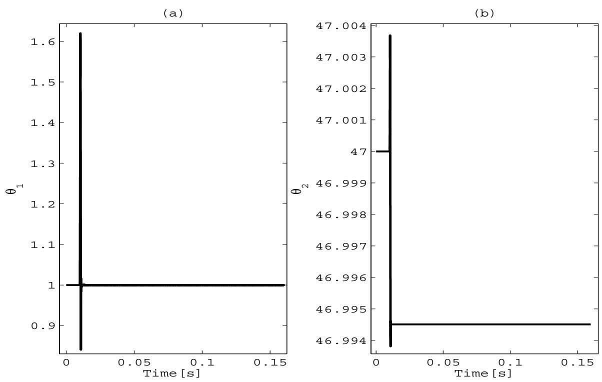

Figure 21: Evolution of adaptation gains θ_1 and θ_2 for change in input voltage and regulator located at feed forward and direct chain.

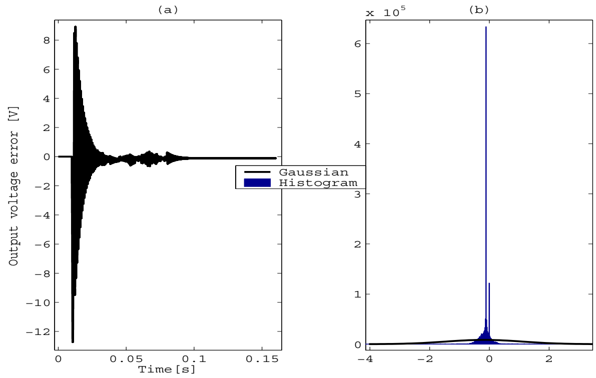

Figure 22: Output voltage error with histogram and Gaussian distribution for change in input voltage and regulator located at feed forward and feed back.

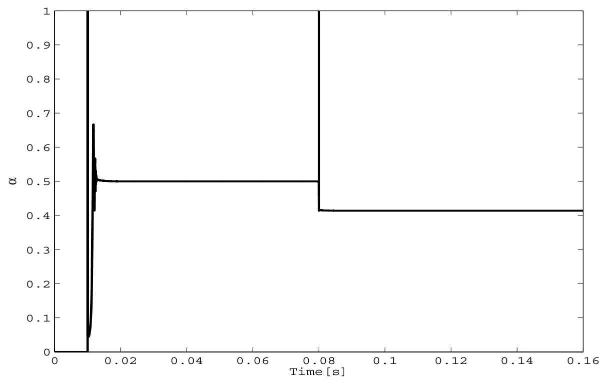

Figure 23: Duty cyclic α for change in input voltage and regulator located at feed forward and feed back.

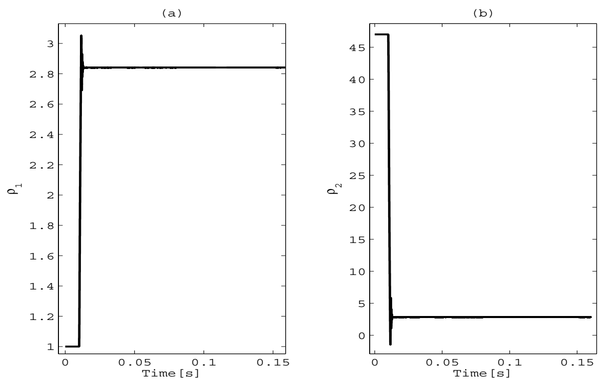

Figure 24: Evolution of adaptation gains ρ_1 and ρ_2 for change in input voltage and regulator located at feed forward and feed back.

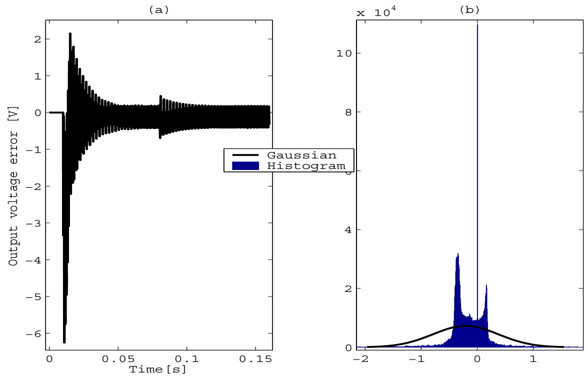

Figure 25: Output voltage error with histogram and Gaussian distribution for change in input voltage and regulator located at direct chain and feed back.

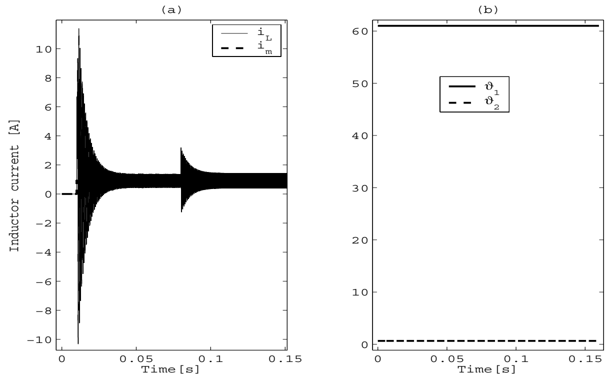

Figure 28: Inductor current with evolution of ϑ_1 and ϑ_2.

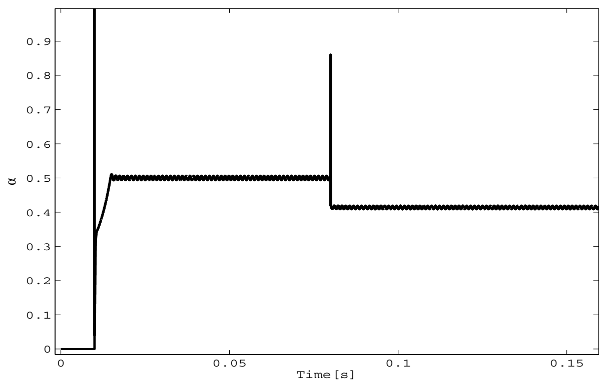

Figure 26: Duty cyclic α for change in input voltage and regulator located at direct chain and feed back.

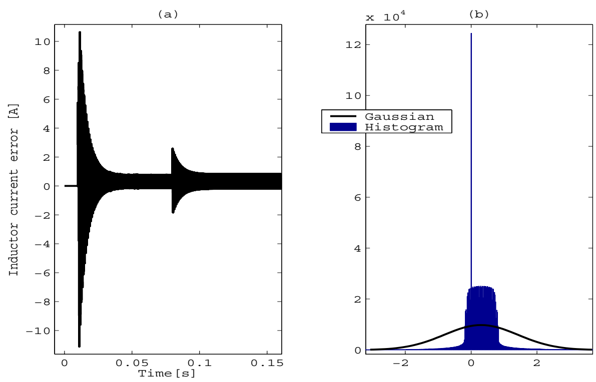

Figure 29: Inductor current error with histogram and Gaussian distribution.

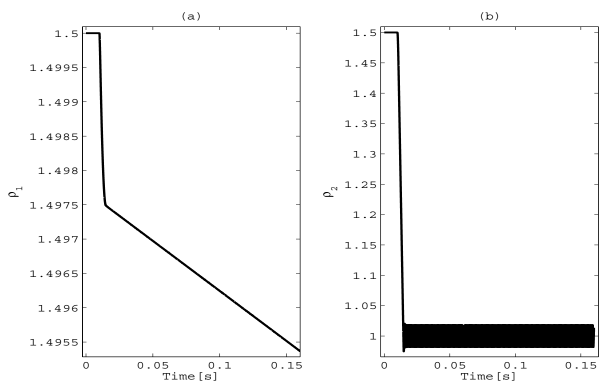

Figure 27: Evolution of adaptation gains ϱ_1 and ϱ_2 for change in input voltage and regulator located at direct chain and feed back.

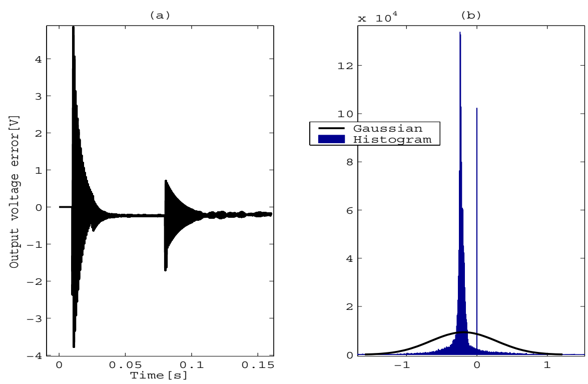

Figure 30: Output voltage error with histogram and Gaussian distribution for change in the resistor load and regulator located at feed forward and direct chain.

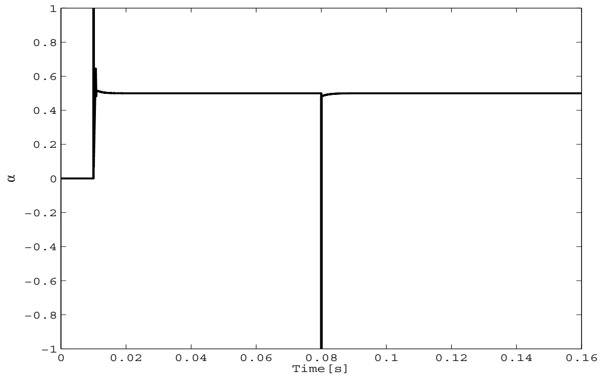

Figure 31: Duty cyclic α for change in the resistor load and regulator located at feed forward and direct chain.

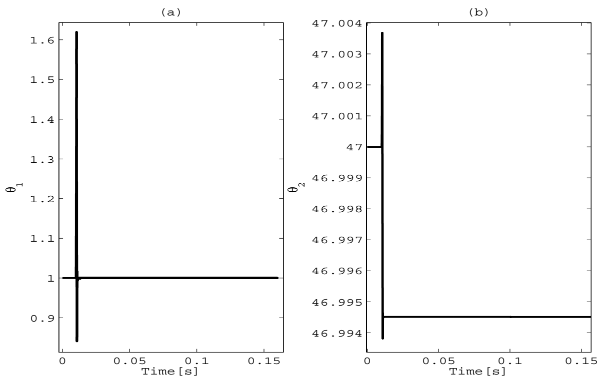

Figure 32: Evolution of adaptation gains θ_1 and θ_2 for change in the resistor load and regulator located at feed forward and direct chain.

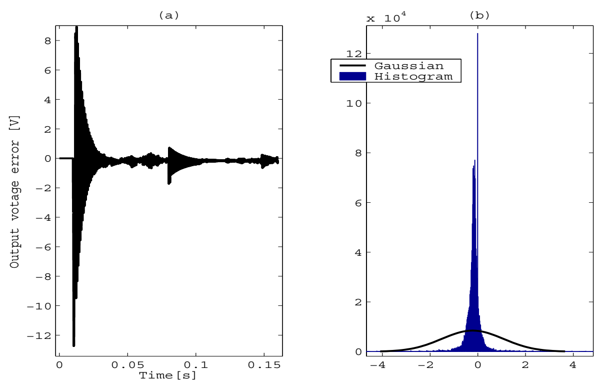

Figure 33: Output voltage error with histogram and Gaussian distribution for change in the resistor load and regulator located at feed forward and feed back.

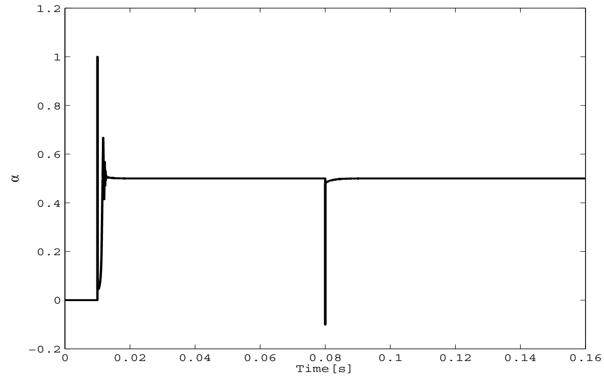

Figure 34: Duty cyclic α for change in the resistor load and regulator located at feed forward and feed back.

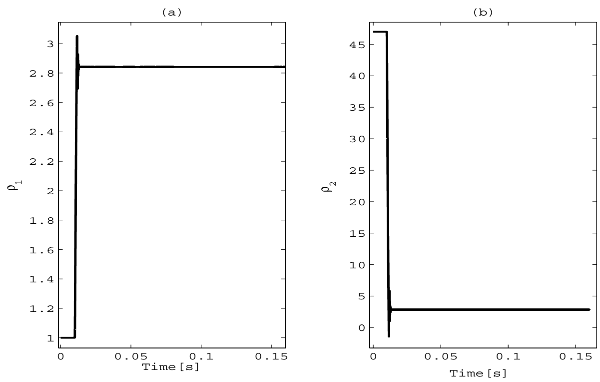

Figure 35: Evolution of adaptation gains ρ_1 and ρ_2 for change in the resistor load and regulator located at feed forward and feed back.

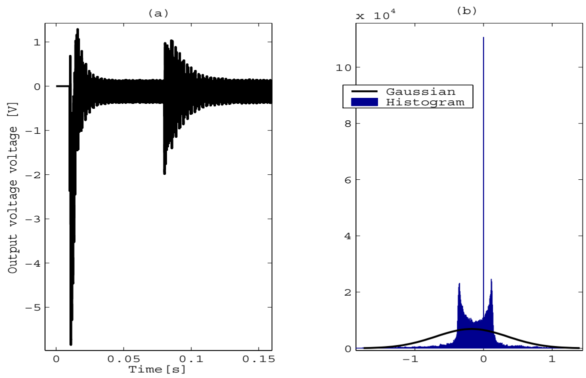

Figure 36: Output voltage error with histogram and Gaussian distribution for change in the resistor load and regulator located at direct chain and feed back.

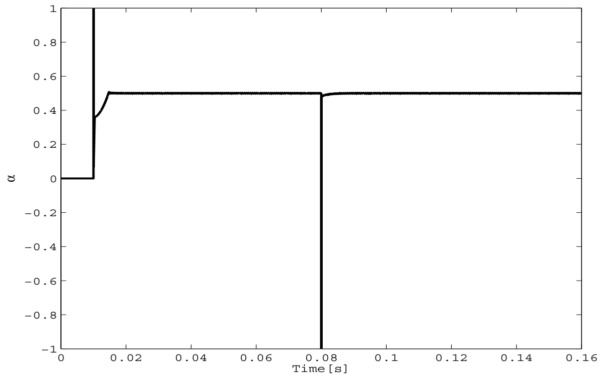

Figure 37: Duty cyclic α for change in the resistor load and regulator located at direct chain and feed back.

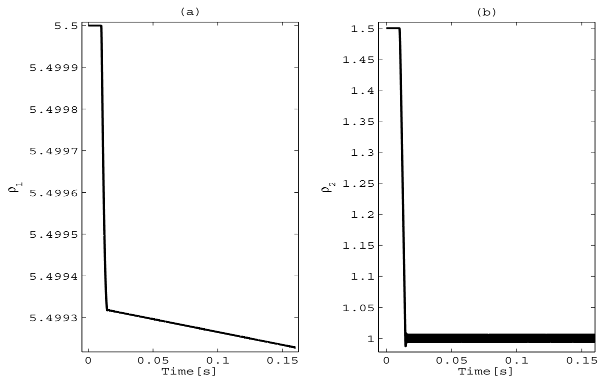

Figure 38: Evolution of adaptation gains ϱ_1 and ϱ_2 for change in the resistor load and regulator located at direct chain and feed back.

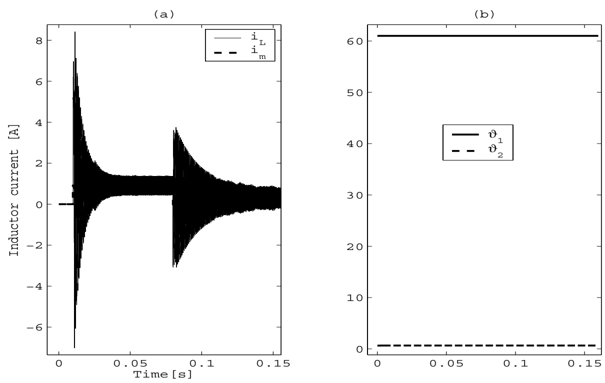

Figure 39: Inductor current with evolution of ϑ_1 and ϑ_2.

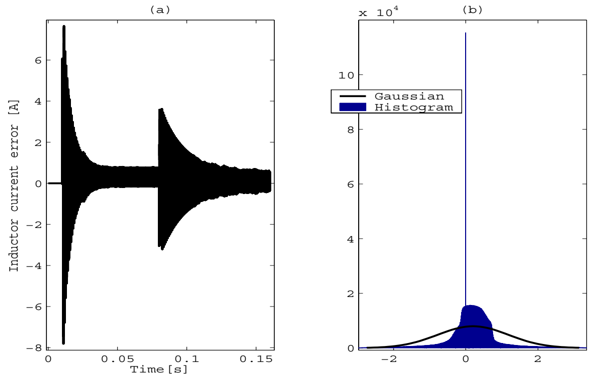

Figure 40: Inductor current error with histogram and Gaussian distribution.

5 Conclusion

In this paper, MRAC is chosen for controlling DC-DC buck converter; where :

- Output voltage regulator located at feed forward and direct chain
- Output voltage regulator located at feed forward and feed back
- Output voltage regulator located at direct chain and feed back

And change for all case in :

- Reference output voltage;
- Input voltage;
- The resistor load.

The smaller mean value obtained, in these assemblies, in the case of the regulator located at the feed forward and direct chain, the change to the input voltage.

References:

[1] C. E. S. Azevedo, Fully Integrated DC-DC Buck Converter, *Lisbonne*, 2015.

[2] M. Biswal, CONTROL TECHNIQUES FOR DC-DC BUCK CONVERTER WITH IMPROVED PERFORMANCE, *Rourkela*, March 2011.

[3] J.-J. Chen, W.-T. Hsu, J.-H. Yu, Y.-S. Hwang and C.-C. Yu, A Fast-Transient-Response Buck Converter with Split-Type III Compensation and Charge-Pump Circuit Technique, *in The 2014 International Power Electronics Conference*, pp:2910-2913, 2014.

[4] C.-C. Chen, C.-H. Huang and S.-C. Tseng, A Fast Transient Response Voltage Mode Buck Converter with an Adaptive Ramp Generator', *International Conference on Information Science, Electronics and Electrical Engineering ICISEEE'14*, 2014.

[5] J.-J. Chen, C.-Y. Huang, C.-I. Chou and C.-C. Yu, A simple fast-transient-response buck converter using adaptive-hysteresis-controlled techniques, *Electron Devices and Solid-State Circuits (EDSSC'15)*, IEEE International Conference, pp:45-48, 2015.

[6] A. Chouya , Commande Adaptative par la Méthode MIT: Théorie et applications', *Editions Universitaires Européennes*, Publié le: 02.12.2020, ISBN-13: 978-620-2-54693-5, ISBN-10: 620254693X, EAN: 9786202546935, https://www.morebooks.shop/store/fr/book/commade-adaptative-par-la-méthode-mit/978-620-2-54693-5

[7] T. Hegarty, Current-Mode Control Stability Analysis For DC-DC Converters, *HOW2POWER TODAY*, pp:1-7, June 2014.

[8] Y.-S. Hwang, A. Liu, Y.-B. Chang and J.-J. Chen, A High-Efficien y Fast-TransientResponse Buck Converter with Analog-Voltage-Dynamic-Estimation Techniques, *IEEE TRANSACTIONS ON POWER ELECTRONICS*, Vol. 30, July 2015.

[9] Y. Liu, C. Zhan and W.-H. Ki, A Fast-Transient-Response Hybrid Buck Converter with Automatic and Nearly-Seamless Loop Transition for Portable Applications, *ESSCIRC*, pp:165-168, 2012.

[10] RMu. Nanda and S. Adhish, Adaptive Control Schemes for DC-DC Buck Converter, *International Journal of enginerring Reseach and Application*, Vol. 2, No. 3, pp.463–467, May-Jun 2012.

[11] D. Spirov, V. Lazarov, D. Roye and Z. Zarkov, Modélisation des convertisseurs statiques DC-DC pour des applications dans les énergies renouvelables en utilisant MATLAB/SIMULINK, *Conférence EF 2009*, UTC, Compiègne, 24-25 Septembre 2009.

[12] N. Sturcken, M. M. Petracca, S. Warren, L. P. Carloni, A. Peterchev and K. L. Shepard, An Integrated Four-Phase Buck Converter Delivering 1A/mm2 with 700ps Controller Delay and Network-on-Chip Load in 45-nm SOI, *Custom Integrated Circuits Conference (CICC'11)*, 19-21 Sept. 2011.

[13] Toni Kotchikpa Arnaud, Conception et intégration d'un convertisseur buck en technologie 28 nm CMOS orientée plateformes mobiles, *THESE de DOCTORAT DE L'UNIVERSITE DE LYON, France*, 10/07/2019, 2019.

[14] P.-Y. Wang, S.-Y. Huang, K.-Y. Fang and T.-H. Kuo, An Undershoot/OvershootSuppressed Current-Mode Buck Converter with Voltage-Setting Control for Type-II Compensator, *IEEE Asian Solid-State Circuits Conference*, Xiamen, Fujian, China, November 9-11,2015.

[15] M. Zelmat, Automatisation des processus industriels : Commande modale et adaptative', *Office des Publications Universitaires*, Tome 2, 2000.

[16] G. Zhou, J. Xu, Y. Jin and J. Sha, Stability analysis of V2 controlled buck converter operating in CCM and DCM, *International Conference on Communications, Circuits and Systems (ICCCAS'10)*, 2010.